

Cross Relaxation between Some Paramagnetic Ions in Crystals Observed by an Optical Method*

C. A. Moore and R. A. Satten

Department of Physics, University of California, Los Angeles, California 90024

(Received 30 August 1972)

An optical-absorption method of monitoring the population changes within the ground Zeeman doublet of paramagnetic ions has been utilized in an optical-microwave double-resonance experiment to measure cross-relaxation effects in mixed crystals. The spin dynamics of the following systems are reported and discussed: Pr-Er(ethylsulfate), Ce-Nd(ethylsulfate), Pr-Ni(double nitrate), and Pr-Sm(ethylsulfate). Experimental results are compared to relevant theories of the spin dynamics and interaction mechanisms which are expected for these ions. The theories of the phonon bottleneck are discussed in terms of their ability to explain some nonexponential decays which are observed in the experiment. A method of estimating the cross-relaxation rate due to virtual-phonon exchange is developed which uses measured spin-lattice relaxation rates to eliminate unknown parameters. The relaxation measurements generally indicate very rapid energy transfer between dissimilar ions which have overlapping resonances, even in a case where the magnetic dipole-dipole interaction is absent.

I. INTRODUCTION

The presence of a spin-spin interaction between different spin species in mixed paramagnetic crystals can cause the observed relaxation time of both species to be altered from their individual rates. To explain such observations, Bloembergen¹ formulated a theory of cross relaxation, introducing the cross-relaxation rate at which spin energy is transferred from one spin species to another. The cross-relaxation rate thus reflects the strength of the spin-spin interaction. Transitions due to the spin-spin interaction are expected to be rapid only when the magnetic splittings of the different ions are similar, i. e., their electron-paramagnetic-resonance (EPR) lines overlap. Interesting relaxation effects result when transitions due to the spin-spin interaction occur at a rate comparable to or greater than the spin-lattice relaxation rate $1/\tau$. The measured relaxation rates of both ions depend on the relative concentration of the ions, the isolated-ion relaxation rates, and the spin-spin interaction rate.

Cross relaxation occurring between paramagnetic ions differs from that occurring between nuclei because of a larger spin-spin interaction and faster spin-lattice relaxation rates. Cross-relaxation effects in electron-paramagnetic systems have usually been observed indirectly by the shortening of spin-lattice relaxation times under circumstances of level crossings between ions with anisotropic splitting factors.²⁻⁴

The phenomenon of cross relaxation has only rarely been investigated for its details because of the inherent experimental difficulties of separately observing the effects on both ions. Microwave double-resonance methods have been successfully

applied to study cross-relaxing ions⁵ and have a resolution capable of investigating different multiple-spin-flip processes. However, such experiments require tunable bimodal cavities and a considerable proliferation of microwave equipment.

An optical-microwave technique has been perfected for the measurement of spin-lattice relaxation of isolated ions, in which the spin population in one of the Zeeman levels of the ground state of the ion is monitored as a function of time after a saturating pulse of microwaves by observing the absorption of circularly polarized light in a transition from the ground state to some excited state of the ion.⁶⁻⁸ This optical technique has features which recommend it for the study of cross relaxation in mixed systems. Because the optical spectra of ions exhibit characteristic line structure, the behavior of two different ions can be separately observed, even though their microwave resonances overlap, by merely choosing the optical-absorption line appropriate to the ion one wishes to monitor. The necessity of using complicated bimodal microwave cavities and the auxiliary electronics is eliminated; however, one must substitute special optical techniques for detection. Finally, because it is a broadband-detection method, the optical method detects cross-relaxation effects between different ionic species only; i. e., the signal for a given ion is free of effects due to cross relaxation between its hyperfine lines and spin diffusion within its line-width.

The selection of suitable ionic systems to study with the optical-absorption method is limited by the requirement that the monitoring circularly polarized light beam must be passed through the crystal parallel to the magnetic field. Since most of the crystals which substitutionally incorporate

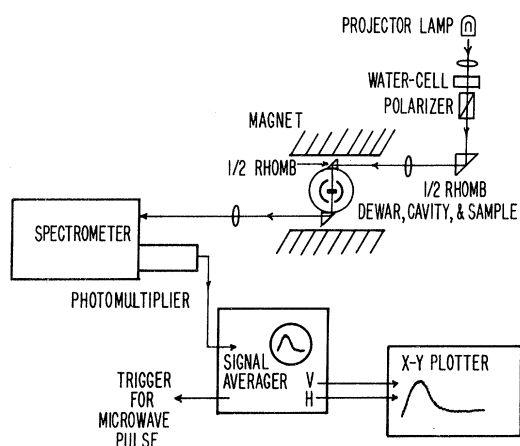


FIG. 1. Diagram of optical equipment. The two right-angle prisms marked $\frac{1}{2}$ rhomb are constructed from glass of the proper index to convert linearly polarized light to circularly polarized light incident on the sample. In combination, these two prisms are equivalent to a Fresnel rhomb.

rare earths are uniaxial, they can transmit circularly polarized light only along the principal axis of the crystal. Thus the selection of ions which are likely to exhibit cross relaxation, and which can be investigated by this optical method, is restricted to those ion combinations which have nearly equal splittings in a magnetic field which is parallel to the crystal axis.

The results of optical-microwave studies of cross-relaxation effects are reported for the following combinations of ions in crystals: praseodymium and erbium in ethylsulfate, cerium and neodymium in ethylsulfate, praseodymium and nickel in double nitrate, and praseodymium and samarium in ethylsulfate.

II. EXPERIMENTAL METHODS

The optical method of monitoring spin populations depends on the existence of selection rules for transitions between quantum states of an ion in a crystal and magnetic field. The selection rules which govern optical transitions between these crystal field states can be obtained in two ways—by perturbation theory or by group theory. The perturbation procedure has been used⁶ to show that, for a given absorption line of neodymium in the ethylsulfate crystal, one of the states of the lowest Zeeman doublet absorbs only right circularly polarized light, while the other absorbs only left-circularly polarized light.

By the methods of group theory, one finds the selection rules are quite generally valid.⁹ The crystal-field-degenerate states which occur for both Kramers and non-Kramers ions in uniaxial crystals have selection rules which require the

two states of a Zeeman doublet in a parallel magnetic field to exhibit complementary behavior with respect to circularly polarized light having one sense of rotation, while the other Zeeman state absorbs circularly polarized light having the opposite sense of rotation.

The optical-microwave method for monitoring spin populations takes advantage of the selection rules in an experiment which is illustrated schematically in Fig. 1. White light from a projector lamp is circularly polarized and passed continuously through the crystal which is polished flat and oriented with its principal axis parallel to the magnetic field and the light path. The crystal is mounted in a microwave cavity which has $\frac{1}{8}$ -in. holes in the walls to pass the focused light through the crystal while it is immersed in a helium bath whose temperature can be controlled between 4.2 and 1.4 °K by pumping. Measurements were generally made only below the λ point of helium at 2.2 °K, where helium bubbles cease to be a source of noise in the light beam. A special Dewar is used which has flat windows and a liquid-nitrogen-free section to pass the light beam without bubble noise from that source. After traversing the crystal, the light beam is reflected out to the spectrometer, which is tuned to an absorption line of the ion to be monitored.

Because of the selection rules, the use of circularly polarized light makes it unnecessary to use an optical spectrometer with resolving power sufficient to resolve the closely spaced Zeeman doublets. A $\frac{1}{2}$ -m Jarrell-Ash spectrometer is used, having slit widths which are variable from 0 to 400 μ , and having a dispersion of 16 Å/mm in first order. This instrument is used to select the optical-absorption line which one wishes to study. Measurements were taken using a slit width of 100 μ for which the optical bandwidth is roughly a factor of 10 wider than the over-all magnetic splitting of the ground state, which for *K*-band measurements is approximately 0.7 cm^{-1} . Thus, the experiment monitors the full width of the microwave resonance, so the signal is unaffected by cross-relaxation effects within the resonance peak or even between hyperfine lines. In this sense, it is different from the microwave methods of observing such phenomena as "hole burning" in the resonance or cross relaxation between hyperfine lines. On the other hand, the optical method can distinguish between different spin species even though their resonances overlap.

Since the optical transitions in rare-earth ions are weak ($f \sim 10^{-7}$), the population of the ground state is not significantly perturbed by the monitoring light beam. This weak transition strength required that these experiments be conducted on samples having a greater concentration of paramagnetic ions

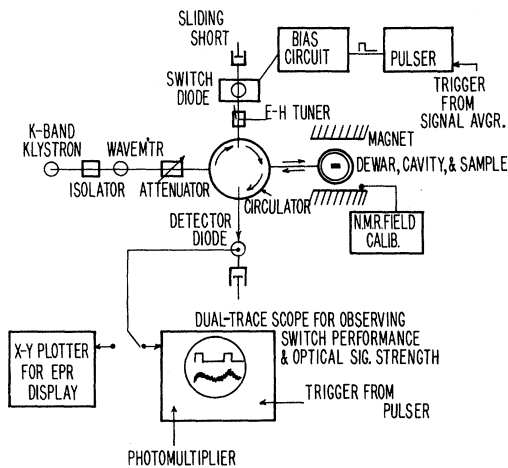


FIG. 2. Diagram of microwave equipment.

than is generally necessary for microwave spectroscopy.

The optical signal observed is the time-resolved response of spin population to a microwave pump pulse and is obtained by tuning the spectrometer to an appropriate optical-absorption line and displaying the light detected by a photomultiplier on an oscilloscope whose sweep is synchronized to the microwave pulse. The signal strength is given by the following expression for the signal-light intensity:

$$I_s = I_0 (e^{-a(N_+^0 + \Delta N_+)x} - e^{-a(N_-^0 + \Delta N_-)x}), \quad (1)$$

where I_0 is the incident left- or right-circularly-polarized-light intensity, N_{\pm}^0 are the values of the population of ions in the upper (+) or lower (-) Zeeman states when in thermal equilibrium with the bath, ΔN are the differences in populations from their equilibrium values at the end of the pump pulse, a is the optical-absorption coefficient, and x is the crystal thickness.

Because the experiment measures a signal impressed on a background of light which is only partially absorbed by the crystal, the major source of noise is the shot noise in the photomultiplier due to its detection of the transmitted light, of which only a portion is the signal. Optimal signal-to-noise ratio occurs when $ax = 2/N_{\pm}^0$; i. e., to achieve the best signal-to-noise ratio, one selects an optical line which absorbs approximately 86% of the light. The signal strength at optimum signal-to-noise ratio is

$$I_s = I_0 e^{-2} (e^{-2\Delta N/N_{\pm}^0} - 1) \approx -I_t (2\Delta N/N_{\pm}^0). \quad (2)$$

One notes that the stronger signal is obtained by using the circular polarization which monitors the upper (+) Zeeman state, and because $\Delta N_+ = -\Delta N_-$, the signal polarity reverses upon reversing the

sense of the light polarization. These characteristics provide a check which can be used to verify that the signal is not of spurious origin such as electronic pickup or bubbling effects in the liquid helium. Spurious bubbling signals were, in fact, encountered when operation was attempted above the λ point of the helium.

A relatively large ΔN was obtained by operating with a microwave frequency of 23.1 GHz (0.77 cm^{-1}). In practice, the ideal signal strength was not always achieved with available microwave power because of fast relaxation times and the large spin concentrations necessary for optimal-optical absorption. Furthermore, some elements (e.g., praseodymium) exist only as isotopes with half-integral nuclear spin having EPR spectra consisting of multiple hyperfine lines. Only one of these could be pumped at a time, whereas the optical absorption arose from all ions. These effects, which diminish the signal strength, in combination with the inherent shot noise, require signal averaging to increase the signal-to-noise ratio. For random-noise processes the signal-to-noise ratio in the average measurement increases as the square root of the number of repeated measurements. A Fabri-tek Instruments model No. FT 1052 signal averager was used which had a 1052 bit memory that could be swept as fast as $50 \mu\text{sec}$ per data point to obtain measurements of decay times as short as $100 \mu\text{sec}$. A thousand repeated measurements were generally required to obtain useful averaged displays.

The microwave apparatus illustrated in Fig. 2 is used both to obtain standard EPR displays of microwave absorption versus field, and to provide microwave pulses of adjustable pulse length. Switching power ratios of 1000:1, with $1\text{-}\mu\text{sec}$ -rise and -decay times, were obtained. After an optical signal was obtained, the pulse width was kept as small as possible to minimize sample-heating effects, and repetition rates were selected which allowed complete relaxation before repulsing.

Two microwave cavities were used in this study. A cylindrical cavity operating in the TE_{011} mode at about 23.2 GHz had vertically oriented magnetic field lines of maximum strength at the center, where the crystal was located; thus, the microwave field was perpendicular to the applied field, and pumped all the Kramers salts. For the non-Kramers salts, pumping by the magnetic field lines of the microwaves is only allowed when the field is parallel to the applied field,¹⁰ so a cylindrical cavity was designed to operate in the TE_{111} mode to provide such a field configuration. Operating at a resonance frequency of 21.2 GHz, this cavity proved useful because it did not efficiently pump the Kramers ions.

EPR displays were obtained by locking the klystron frequency to that of the cavity with an auto-

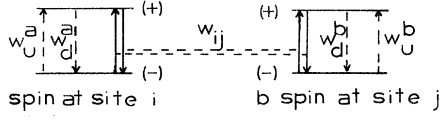


FIG. 3. Illustration of cross-relaxing levels and rates. w_u and w_d indicate relaxation transitions and w_{ij} indicates interaction transitions. The optical method can be used to separately observe the population in any of the four levels shown.

matic-frequency-control circuit and recording χ'' vs field on the x - y plotter. Optical spectra were recorded using the same optical setup as for the relaxation measurements. The relaxation measurements were then made as a function of temperature and of position on the χ'' versus field curve at which microwave pumping was applied. The decay curve in the memory of the signal averager was read out to an x - y plotter to be later replotted on semilog paper to determine the characteristic of the decay.

Crystals which accommodate rare-earth ions in substitutional sites are desirable to allow freedom to vary the relative concentration of the ions without problems of charge compensation. In addition, for the study of cross relaxation, prior work done to understand the optical spectra, EPR, and spin-lattice relaxation is useful, although this data had to be retaken with each sample. The two crystals chosen satisfy these criteria. They are the ethyl-sulfates and the double nitrates, which are dilute magnetic structures having the respective chemical formulas $R(C_2H_5SO_4)_3 \cdot 9H_2O$ and $R_2T_3(NO_3)_{12} \cdot 24H_2O$, where R represents a rare-earth ion or the diamagnetic lanthanum ion, and T represents a divalent transition-metal ion, or the diamagnetic magnesium ion.

III. THEORY

A. Cross Relaxation

The rate equations for cross relaxation in mixed systems, such as between the levels illustrated in Fig. 3, were originally formulated by Bloembergen.¹ The rate equations which describe the populations of all four levels under the influence of both spin-flip processes and ordinary relaxation processes are

$$\dot{N}_a^+ = -\dot{N}_a^- = \sum_{j=1}^{N_b} w_{ij} \left(-N_a^+ \frac{N_b^-}{N_b} + N_a^- \frac{N_b^+}{N_b} \right) + w_u^a N_a^- - w_d^a N_a^+, \quad (3a)$$

$$\dot{N}_b^+ = \sum_{i=1}^{N_a} w_{ij} \left(-N_b^+ \frac{N_a^-}{N_a} + N_b^- \frac{N_a^+}{N_a} \right) + w_u^b N_b^- - w_d^b N_b^+, \quad (3b)$$

where N_b^-/N_b is the probability that the (-) state of

the b -type ion at site j is populated, and w_u and w_d are spin-lattice transition rates. w_{ij} is a transition rate for mutual spin-flip processes given by

$$w_{ij} = \hbar^{-2} | \langle E_i, E_j | H_{ij} | E_i + h\nu_a, E_j + h\nu_b \rangle |^2 g_{ab}(\nu), \quad (4)$$

where H_{ij} represents the "spin-flip" portion of any effective spin-spin interaction—one example of which is the magnetic dipole-dipole interaction—and where $g_{ab}(\nu)$ is an overlap function for the resonances, which gives the probability that the spin system can absorb excess Zeeman energy $h(\nu_a - \nu_b)$. For Gaussian line shapes, Bloembergen evaluates the overlap function to be

$$g_{ab} = [2\pi(\Delta\nu_a^2 + \Delta\nu_b^2)]^{-1/2} \times \exp[-(\nu_a - \nu_b)^2 / 2(\Delta\nu_a^2 + \Delta\nu_b^2)], \quad (5)$$

where $\Delta\nu_a$ and $\Delta\nu_b$ are the halfwidths of the line shapes, and ν_a and ν_b are their centers. The spin-flip Hamiltonian for two spins can be expressed as

$$H_{ij} = [(g_{ij}^a g_{ij}^b / 2R_{ij}^3) + B_{ij}] (S_i^+ S_j^- + S_i^- S_j^+), \quad (6)$$

where B_{ij} is the coefficient for the nondipolar interactions.

When expressed in terms of the total populations $N_a = N_a^+ + N_a^-$ and population differences $n_a = N_a^- - N_a^+$, the rate equations become the following coupled linear differential equations with constant coefficients^{3,4}:

$$\dot{n}_a = W(N_a n_b - N_b n_a) - (n_a - n_a^0) r_a, \quad (7a)$$

$$\dot{n}_b = W(N_b n_a - N_a n_b) - (n_b - n_b^0) r_b, \quad (7b)$$

where $r_a = w_u^a + w_d^a$ is the spin-lattice relaxation rate for a spins and

$$W = N_b^{-1} \sum_{j=1}^{N_b} w_{ij} = N_a^{-1} \sum_{i=1}^{N_a} w_{ij}. \quad (8)$$

These equations are solved to give the following result for the populations as a function of time:

$$n_a(t) = A_+ e^{-r_+ t} + A_- e^{-r_- t} + n_a^0, \quad (9a)$$

and

$$n_b(t) = B_+ e^{-r_+ t} + B_- e^{-r_- t} + n_b^0, \quad (9b)$$

where, if a cross-relaxation rate is defined by

$$r_{ab} \equiv W(N_a + N_b) = \left(1 + \frac{N_b}{N_a} \right) \sum_{i=1}^{N_a} w_{ij}, \quad (10)$$

then

$$r_{\pm} = \frac{1}{2} \{ (r_{ab} + r_a + r_b) \pm [r_{ab}^2 + (r_b - r_a)^2 2r_{ab}(r_b - r_a) \times (N_a - N_b / N_a + N_b)]^{1/2} \}, \quad (11)$$

$$A_{\pm} = \pm (1/r_+ - r_-) [n_a(0) - n_a^0] (r_a - r_{\pm})$$

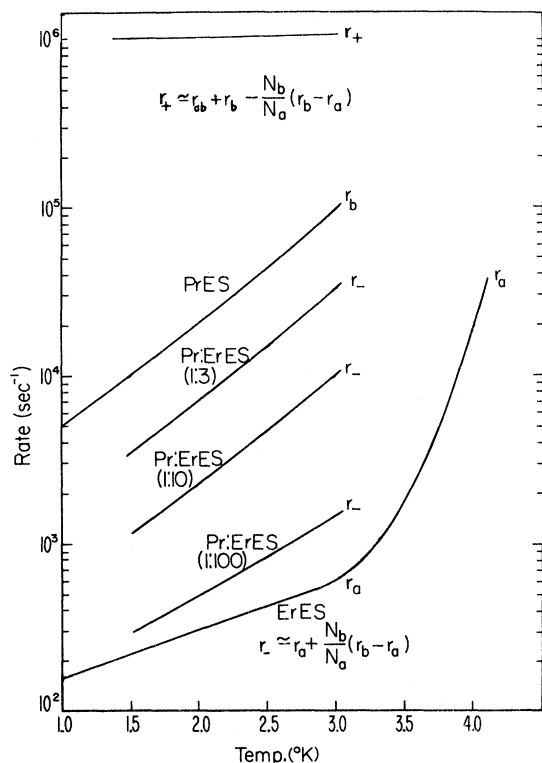


FIG. 4. Temperature dependence of the relaxation rates predicted by the cross-relaxation equations (13a) and (13b) for some mixed crystals of praseodymium-erbium ethylsulfate if r_{ab} is assumed to be 10^6 sec^{-1} (case I). The rates for the isolated ions have been taken from Larson and Jeffries (Ref. 30). The rate for the direct process in erbium has been extrapolated by the expected ω^4 dependence to give a rate predicted for the microwave cavity used here. The rate for praseodymium has not been extrapolated as it was phonon bottlenecked.

$$+ n_a(0)WN_b - n_b(0)WN_a \} , \quad (12)$$

and B_* is the same expression with a and b subscripts interchanged.

The decay of each type of ion is thus a compound exponential with rates r_+ and r_- , and having a dominant contribution from the slow r_- rate. Since $r_+ + r_- = r_{ab} + r_b + r_a$, if both r_+ and r_- were measured, knowledge of r_a and r_b is sufficient to determine r_{ab} independent of the relative concentration of the ions.

Interesting results occur for two cases when $N_a > N_b$.

Case I. When $r_{ab} > r_b - r_a$, then

$$r_- \approx r_a + (r_b - r_a)(N_b/N_a) \quad (13a)$$

and

$$r_+ \approx r_{ab} + r_b - (r_b - r_a)(N_b/N_a) . \quad (13b)$$

Figure 4 shows, as an illustration of this case, the

relaxation rates which would be expected for Pr-Er ethylsulfates if it is assumed $r_{ab} = 10^6 \text{ sec}^{-1}$.

Case II. When $r_{ab} < r_b - r_a$, then

$$r_- \approx r_a + r_{ab}(N_b/N_a) \quad (14a)$$

and

$$r_+ \approx r_b + r_{ab}(1 - N_b/N_a) . \quad (14b)$$

Figure 5 shows, as an illustration of this case, the relaxation rates which would be expected for Pr-Er ethylsulfates if $r_{ab} = 10^3 \text{ sec}^{-1}$.

The experiments reported here did not allow a complete fit to all the coefficients and rates which appear in the expressions for $n_a(t)$ and $n_b(t)$. The initial populations at the onset of decay were not known, and the time response of the signal averager did not permit observation of the fast decay r_+ . Furthermore, the presence of phonon heating confused the problem by introducing more rates. However, Figs. 5 and 6 illustrate that observation of only the slower relaxation rate in a series of crystals permits a direct determination of r_{ab} in case II, while in case I a lower limit, $r_{ab} > r_b - r_a$, can be inferred.

Since in the application of Eq. (4) neither the val-

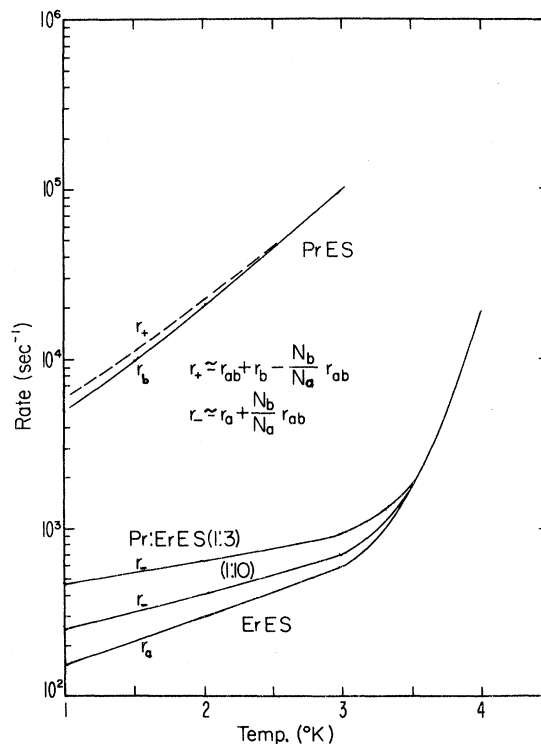


FIG. 5. Temperature dependence of the relaxation rates predicted by the cross-relaxation equations (14a) and (14b) for some mixed crystals of praseodymium-erbium ethylsulfate if r_{ab} is assumed to be 10^3 sec^{-1} (case II).

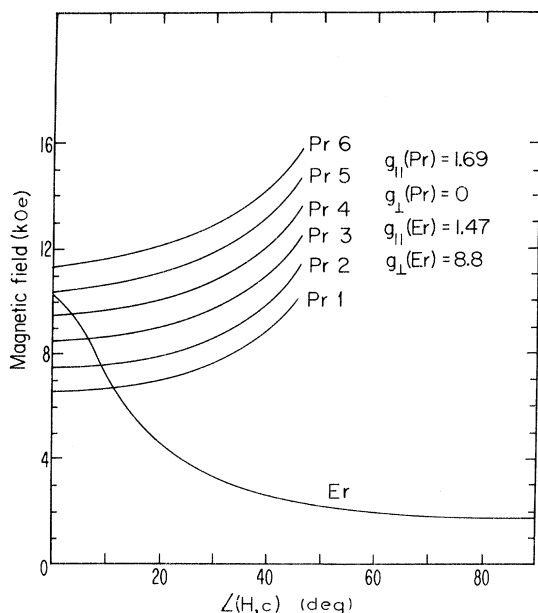


FIG. 6. Predicted angular dependence of the microwave-resonance absorption for Pr and Er ions in the ethylsulfate crystal for a cavity frequency of 21.2 GHz. g values are from Ref. 26.

ue of the matrix element nor the proper value of the overlap function is known in specific cases, one must be satisfied with order-of-magnitude estimates of cross-relaxation rates. The matrix element can have contributions from a number of different interactions which will be discussed later. The proper value of the overlap function is difficult to obtain in the samples studied here because the EPR spectra are complicated by the presence of the hyperfine structure and pair structure, and by the well-known inhomogeneous line shape of the non-Kramers ions.

A rough estimate of g_{ab} can be obtained using Eq. (5) which, when evaluated for complete overlap of two Gaussians with a width appropriate for the concentrated samples studied here (100 G), gives $g_{ab} \approx 10^{-9}$ sec. Then, $w_{ij} \approx 10^{13} |H_{ij} \text{ cm}^{-1}|^2$. Thus any interaction having matrix elements as weak as 10^{-4} cm^{-1} is sufficient to give a cross-relaxation rate $\tau_{ab} \approx 10^5 \text{ sec}^{-1}$, faster than most spin-lattice relaxation rates encountered in rare earths at low temperatures

As the estimates in Sec. III B show, even the weakest interactions between neighboring rare-earth ions are sufficiently strong to give, for overlapping resonances, relaxation behavior which is characteristic of case I rather than case II.

B. Interaction Mechanisms

It has been found that the principal contribution to the interactions between rare-earth ions in

ethylsulfates is attributable to the easily calculated magnetic dipole-dipole interaction. Work on the EPR of the concentrated salts and on pair spectra¹¹⁻¹⁶ has shown evidence of additional contributions from other interactions. The important ones are thought to be (i) the interaction of the electric multipoles of the charge distributions which characterize the ions, and (ii) the virtual-phonon-exchange (VPE) interaction, a second-order process which couples the two ions by the emission and absorption of pairs of phonons. These additional interactions are important in the study of cross relaxation when one of the ions has $g_{\perp} = 0$, for the magnetic dipole-dipole interaction then lacks the terms in $S_i S_j$ which cause cross relaxation. The original papers which treated electric multipole interactions (EMI) used only the first effective term in the expansion of the electro-static interaction, the electric quadrupole-quadrupole term (EQQ), as successive terms were expected to fall off as r^2/R_{ij}^2 , where r is the electronic radius and R_{ij} is the ionic separation.^{17,18} However, Wolf and Birgeneau,¹⁹ having studied numerous pair spectra in the trichlorides, assert that, as in the case of crystal field parameters, the higher-order terms may be equally effective as the second-order-EQQ terms because of shielding and ligand polarizability effects. They suggest that the problem of interactions between pairs of ions be treated by an effective spin-spin Hamiltonian whose coefficients are not directly calculated, but empirically determined.

Detailed calculations of the EQQ have been reported. The calculations for Kramers ions are ponderous because the interaction, no matter how low its symmetry, cannot connect in first order the time-reversed states of a Kramers doublet. The interaction is therefore calculated in second order involving excited states of the ground manifold of the ion. The calculations of the EQQ in Ce ethylsulfate (ES) by Dweck and Seidel,¹² when corrected for an error in their value for $\langle r^2 \rangle$, indicate that the EQQ is of insufficient strength to give their measured line shift. Baker's work on NdES and CeES also indicates that EQQ alone is insufficient to explain his measured line shifts.^{13,14}

Table I summarizes the magnitude of dipolar interactions and some reported nondipolar line shifts for ethylsulfate crystals. As an indication of the order of magnitude of the off-diagonal contributions, these line-shift measurements indicate that nondipolar interactions are of sufficient strength to cause rapid cross-relaxation rates.

It is still not clear, however, if the nondipolar interactions are attributable to higher-multipole interactions or to VPE.^{15,19} Orbach and Tachiki²⁰ developed a theory of the VPE in a formulation similar to that of spin-lattice relaxation theory. One of the processes they discuss is a resonant in-

TABLE I. Interaction strengths of the rare-earth ions in ethylsulfates. Magnitude of the magnetic dipolar interaction between nearest-neighbor ions in ethylsulfate crystals, and some nondipolar line shifts measured in the EPR spectra. Values are in wave numbers.

Ion pair	$-\frac{2g_{\parallel}^a g_{\parallel}^b \mu_B^2}{R_{ij}^3 \hbar c}$	$\frac{g_{\perp}^a g_{\perp}^b \mu_B^2}{R_{ij}^3 \hbar c}$	Measured nondip	Ref.
Ce-Ce	-0.034	4.6×10^{-5}	0.105 0.113	14 12
Ce-Nd	-0.032	4.8×10^{-4}	0.013	12
Nd-Nd	-0.030	0.005	0.001	13
Pr-Er	-0.015	0
Tb-Tb	-0.762	0	0.013	20
Ho-Ho	-0.578	0	0.002	20
Dy-Dy	-0.285	0	0.003	20

interaction which involves the two ions and those phonons having an energy equal to the Zeeman splitting of the ions. They derive the following expression for the matrix element of the VPE interaction which applies under the conditions of this experiment ($R_{ij} < 1/k_{\delta}$, and $\delta < \hbar\omega_{\text{Debye}}$):

$$M \approx \frac{3}{8\pi\rho v^2 R_{ij}^3} \sum_{n,n',m} V_n^m(i) V_{n'}^m(j), \quad (15)$$

where δ is the Zeeman splitting, ρ is the density of the crystal, v is the velocity of sound in the crystal, $1/k_{\delta} = \hbar v / \delta$, and $V_n^m(i)$ are matrix elements of the electron-vibrational interaction acting at site i .

Using the values $v = 2 \times 10^5$ cm/sec, $R_{ij} = 7.1 \text{ \AA}$, and $\rho = 1.8$ g/cm³, and converting the expression (15) to units of cm⁻¹, one finds for the nearest neighbors in the ethylsulfates,

$$M \approx 9 \times 10^{-7} \sum_{n,n',m} V_n^m(i) V_{n'}^m(j), \quad (16)$$

where the $V_n^m(i)$ matrix elements are measured in cm⁻¹. Applied to the case of the rare-earth ions, n and n' are even and ≤ 6 . One expects terms in all $|m| < n$ to characterize the vibrating lattice. As in the case of direct-process relaxation, this interaction cannot connect the time-reversed states of a Kramers ion in first order, and the admixture of excited states is necessary for a nonvanishing result. If admixture is accomplished via the magnetic field, one expects the VPE between Kramers ions to be reduced in comparison to that between non-Kramers ions by a factor of δ^2/Δ^2 , where δ is the Zeeman splitting (~ 1 cm⁻¹), and Δ is the energy of the excited state (~ 10 cm⁻¹).

Estimating $V_n^m(i) = 10$ cm⁻¹ and $\delta/\Delta \sim 10^{-1}$, one finds for the VPE

$$M(\text{Kramers}) = 10^{-6} \text{ cm}^{-1}$$

and

$$M(\text{non-Kramers}) = 10^{-4} \text{ cm}^{-1}.$$

This is of sufficient strength to contribute to a rapid cross-relaxation rate. Since the VPE can have effective matrix elements up to $|m| = 6$, it may be more effective than the EQQ for some ions.

The expression for the rate of cross relaxation suggests a new method for the estimation of the effectiveness of the VPE in causing cross relaxation. Because the VPE for Zeeman energies has its major contribution from those phonons with energy δ , one suspects that an estimate of its contribution to the cross-relaxation rate may be obtained from the spin-lattice relaxation rate of the direct process. Such an estimate eliminates the necessity of using the estimates^{21,22} of the numerous V_n^m parameters which appear in both spin-lattice relaxation theory and the theory of the VPE.

The expression for the rate of cross relaxation due to the virtual-phonon exchange is

$$w_{ij}^{\text{VPE}} = \frac{9}{64\hbar^2 \pi^2 \rho^2 v^4 R_{ij}^6} \sum_{n,n',m} \left(V_n^m(i) V_{n'}^m(j) \right)^2 g_{ab}(v), \quad (17)$$

while the expression for the spin-lattice relaxation by the direct process for a non-Kramers salt is

$$\tau^{-1} = \frac{3}{2\pi\rho v^5 \hbar} \left(\frac{\delta}{\hbar} \right)^3 \sum_{n,m} \left(V_n^m(i) \right)^2 \left(\frac{2kT}{\delta} \right). \quad (18)$$

Thus, as an order-of-magnitude estimate which neglects phonon correlation,

$$w_{ij}^{\text{VPE}} \approx |\tau_a^{-1} \tau_b^{-1}|_{\text{Direct}} (\hbar^6 v^6 / 64k^2 R_{ij}^6) (\delta^4 T^2)^{-1} g_{ab}(v), \quad (19)$$

where the experimentally measured spin-lattice rate now takes the place of the undetermined matrix elements. This estimate is expected to hold for Kramers salts, assuming that the VPE operates through admixtures by the magnetic field. This expression for w_{ij} is properly independent of the temperature at which $1/\tau$ is measured, since the direct process varies linearly with T .

Applying this estimate to the nearest neighbors in ethylsulfates and using the parameters $v = 2 \times 10^5$ cm/sec, $T_0 = 1.5$ °K, $R_{ij} = 7.1 \times 10^{-8}$ cm, and $\nu_0 = \delta/\hbar = 23.1$ GHz, one finds for an overlap $g_{ab} \approx 10^9$ sec,

$$w_{ij}^{\text{VPE}} = 7 \times 10^{-3} [\tau_a \tau_b]_{T_0, \nu_0}^{-1}. \quad (20)$$

C. Phonon Bottleneck

The phonon bottleneck is a phenomenon commonly accompanying relaxation of paramagnetic ions by the direct process. It is a manifestation of a sharp increase in the number of phonons having an energy corresponding to the Zeeman splitting of the relaxing ions. The resulting peak in the number of phonons versus energy curve can be described in terms of a higher effective temperature for the phonons in a band corresponding to the bandwidth of the spins. Such a peak of phonons, if there were

no spins continuing to feed it, would have a relaxation time much shorter than the characteristic relaxation times of paramagnetic ions. It is only because the number of spins exceeds so greatly the ambient number of acoustic phonons in that bandwidth that the combined system of spins and phonons exhibits a longer "bottlenecked" relaxation time.

The rate equations for spins and phonons have been treated by Faughnan and Strandberg,²³ Scott and Jeffries,²² and Stoneham.²⁴ These treatments will be discussed here for the purpose of interpreting the data.

The rate equations for spin-population difference n and phonon average occupation number \bar{p} , when written in terms of $(n - n_0)$ and $(\bar{p} - \bar{p}_0)$, where the 0 subscript designates thermal equilibrium at the bath temperature, are²²

$$\dot{n} = -\frac{n - n_0}{\tau} - \frac{n(\bar{p} - \bar{p}_0)}{\tau(\bar{p}_0 + \frac{1}{2})}, \quad (21a)$$

$$\dot{\bar{p}} = \frac{-\sigma(\bar{p}_0 + \frac{1}{2})(n - n_0)}{\tau_p n_0} - \frac{[\sigma(n/n_0) + 1](\bar{p} - \bar{p}_0)}{\tau_p}, \quad (21b)$$

where τ is the direct-process spin-lattice relaxation time, τ_p is the phonon-bath relaxation time, and the bottleneck factor σ is defined by

$$\sigma \equiv \frac{\tau_p n_0}{2\tau(\bar{p}_0 + \frac{1}{2}) \Delta\delta\rho(\delta)} = \frac{E_s/\tau}{E_p/\tau_p}, \quad (22)$$

in which E_s and E_p are the energies of the spin and phonon system, respectively, and $\rho(\delta)$ and $\Delta\delta$ are the phonon density and the spin bandwidth.

Scott and Jeffries linearize these equations by setting $n = n_0$ in the coefficients of $\bar{p} - \bar{p}_0$ and thus obtain a solution which is valid only in the tail of the relaxation where $n - n_0 < 1$. These linearized equations can be solved to obtain two rates which are valid to first order in τ_p/τ :

$$b_+ = 1/\tau(\sigma + 1), \quad (23a)$$

$$b_- = \frac{\sigma + 1}{\tau_p} + \frac{\sigma}{\tau(\sigma + 1)}. \quad (23b)$$

The b_+ solution is the commonly seen bottlenecked rate which gives significant departures from $1/\tau$ for $\sigma > 1$. Using the expression for σ , the familiar T^2 dependence for the strongly bottlenecked rate yields, for $kT > \delta$ and $\sigma > 1$,

$$b_+ \approx \frac{1}{\tau\sigma} = \frac{6\Delta\delta k^2}{\tau_p \pi^2 c v^3 \hbar^3} T^2 = DT^2. \quad (24)$$

In the intermediate ($\sigma \approx 1$) case, the T dependence is mixed:

$$b_+ = DT^2/[1 + (D/A)T], \quad (25)$$

where $1/\tau = AT$ is the unbottlenecked direct-process spin-lattice relaxation rate. These conclusions are very useful for recognizing the presence

of a phonon bottleneck.

The b_- solution, which is essentially the phonon relaxation rate modified by the coupling to the spins, does not appear in full detail in the literature. However, its leading term for $\sigma \gg 1$ is σ/τ_p , and is estimated by Scott and Jeffries to be quite fast. Equations (23) can be solved to give τ_p in terms of the two rates b_+ and b_- .

Nonexponential-decay curves were observed in this experiment (for the Ce and Nd ions in the ethylsulfates) which could not be attributed to cross relaxation. If these nonexponential decays were fit to a sum of two exponentials, the two rates did not differ by more than an order of magnitude from τ^{-1} . If these two experimental rates were to be identified with the b_- and b_+ of the linearized equations, then τ_p would have to be of the same order of magnitude as τ . This is much longer than the values of τ_p of 10^{-6} – 10^{-7} sec estimated for the ethylsulfates.^{23,24} This result, in addition to the restricted validity of the linearized equation to spin populations near thermal-equilibrium values, leads to the conclusion that it is inappropriate to attempt to apply the solutions of the linearized equations to nonexponential decays which arise when initial spin populations may approach saturation.

The Stoneham analysis of the phonon bottleneck is a thermodynamic approach cast in terms of the spin, lattice, and bath temperatures, T_s , T_L , and T_B .²⁴ Starting with linear equations, he obtains $\tau(\text{observed}) = \tau + \tau_p(c_s/c_p)$, which is equivalent to the b_+ rate of Scott and Jeffries. By solving the linear Stoneham equations, one obtains the same solutions b_- and b_+ , showing the equivalence of Stoneham's thermodynamic approach to the Scott and Jeffries linearized equations in which the assumptions are more clearly introduced.

Faughnan and Strandberg's analysis of the coupled spin-phonon equations avoids the linearization process, which resulted naturally in the solution in terms of two time constants, and it gives solutions whose validity is not restricted to the tail of the relaxation. Their procedure is to solve the nonlinear-coupled equations numerically. In addition, they obtain a transcendental expression as an approximation which, by direct comparison with the numerical results, is found to be quite accurate in all cases where the bottleneck factor is of order unity. In particular, the approximate expression is in agreement with their numerical results for values of n departing significantly from n_0 , i. e., near saturation. It was found that the approximate expression was useful to predict the appearance of nonexponential decays for values of σ of order unity.

Faughnan and Strandberg predict for values of σ of order unity a clearly detectable nonexponential decay with an initial slope τ^{-1} and final slope

$[(\sigma + 1)\tau]^{-1}$. In their treatment of the spin-phonon equations, the observation of such departures from exponentiality does not require the conclusion that τ_{phonon} is of the order of magnitude of τ_{spin} .

IV. EXPERIMENTAL RESULTS

A. Praseodymium-Erbium Ethylsulfates

The ethylsulfate crystal doped with praseodymium (f^2) and erbium (f^{11}) ions is a suitable candidate for the study of cross relaxation because of overlapping resonances. Figure 6 shows the expected angular dependence of the paramagnetic-resonance spectra. The praseodymium ion exists in nature only with a nuclear spin $I = \frac{5}{2}$, so its resonance spectrum consists of six hyperfine lines which exhibit the characteristic broad asymmetric line shape of non-Kramers ions.^{18,25}

The erbium ion has a resonance position which varies greatly with the angle θ , which the external field makes with the crystal axis. In particular, near $\theta = 0$, where the optical technique is used, the extent of overlap of the erbium resonance with those of the praseodymium ion is very sensitive to small changes in the angle of magnetic field. The erbium ions are pumped by the conventional $\vec{h} \perp \vec{H}$ geometry, and the large value of g_{\perp} for erbium causes a broad and strong EPR spectrum in crystals containing high concentrations of this ion.

A TE_{111} cavity was constructed to obtain a field configuration having h parallel to the optical holes at the bottom of the cavity where the crystal was located. Magnetic-resonance measurements taken with this cavity showed absorptions due to the praseodymium ions, and an erbium absorption of increasing intensity as the magnetic field was rotated away from $\theta = 0$. This cavity was generally used for cross-relaxation measurements because it allowed pumping of praseodymium hyperfine lines which had little overlap with erbium ions.

Relaxation measurements for isolated erbium and praseodymium ions in ethylsulfates were obtained by Larson and Jeffries⁴ at X band. At low temperatures the erbium ion exhibits the slow relaxation rate characteristic of the direct process in Kramers ions. Measurements made in this study on erbium ethylsulfate at K band agreed with the rate predicted by extrapolating the Larson and Jeffries rate by the ω^4 dependence of spin-lattice relaxation theory.

Above the λ point of helium, the optical decay was seen to exhibit large oscillatory behavior which was not the same in successive averaged displays, and was independent of the circular polarization used, always being absorptive in nature. This is believed to be caused by bubbling at the surface of the crystal. Below the λ point, the signal of all the samples showed the expected reversal of signal polarity with the circular polarization; that is, the

upper Zeeman state exhibits increased optical absorption after the microwave pulse, while the transition from the lower Zeeman state exhibits decreased absorption. As expected from the signal-strength analysis, the signal from the upper state was always larger than the signal from the lower state.

Praseodymium exhibits the rapid relaxation behavior characteristic of non-Kramers ions. At K-band frequencies it was found to have a rate roughly 15 times faster than erbium, and having the temperature dependence of the phonon bottleneck, fitting the expression $1/\tau = 2 \times 10^9 T^2 \text{ sec}^{-1}$.

Ethylsulfate crystals containing both praseodymium and erbium were grown from water solution. As there was a marked tendency for the ions to segregate during crystallization, the relative concentration of the ions had to be estimated from the optical-absorption spectra. Crystals having erbium, as the more abundant ion, were preferred as the relaxation times were then longer, and the optical spectra of both ions then exhibited absorption strengths near the value necessary for best signal to noise. Figure 7 shows the results of some relaxation measurements made on crystals containing praseodymium doped into erbium ethylsulfate, along with data on pure erbium ethylsulfate and praseodymium-doped lanthanum ethylsulfate. Figures 8 and 9 show microwave-absorption data for the mixed samples which indicate the relative linewidths of the resonances. The praseodymium hyperfine lines are labeled Nos. 1-6, a designation used hereafter. In this ErES host, the praseodymium resonances exhibited a g value of 1.5, much closer to the 1.52 value characterizing

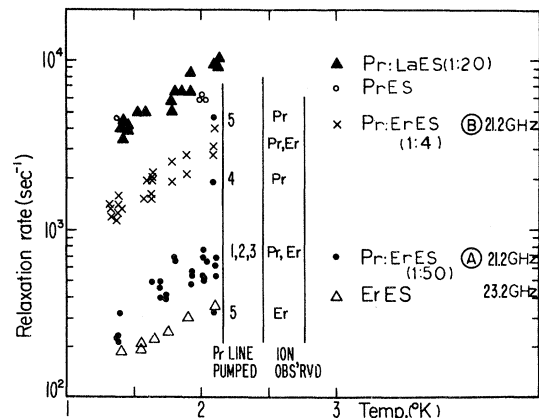


FIG. 7. Temperature dependence of the observed relaxation rates in Pr:ErES crystals having differing relative concentrations for Pr and Er ions. Relative concentrations are indicated in parentheses. Next to the corresponding data, information is given indicating which of the hyperfine lines were pumped by microwaves and which ions were observed by the optical method.

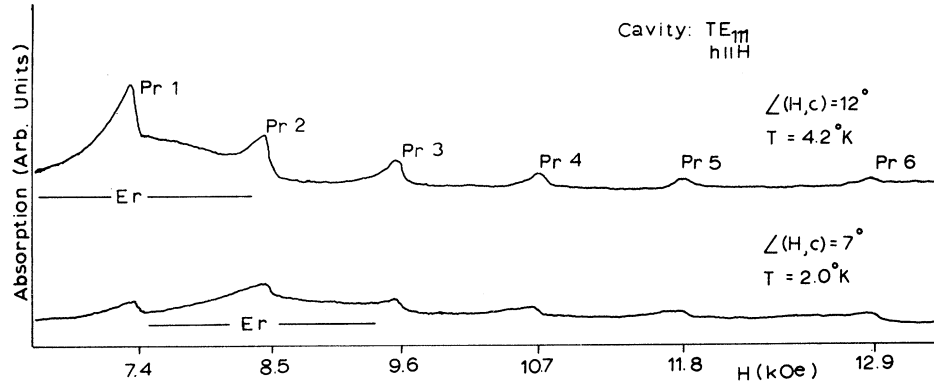


FIG. 8. Microwave-absorption spectrum of the Pr:ErES (1:50), sample A.

Pr in yttrium ethylsulfate²⁵ than the value 1.69, which was observed for Pr in lanthanum ethylsulfate.¹⁰

With microwave pulses applied at fields where the resonances overlapped significantly, the relaxation of both the Er optical lines and the Pr lines were the same to within experimental error, and exhibited exponential decay. This is an indication of a tight coupling of Pr and Er ions where their resonances overlap.

One obtains information about the cross-relaxation rate by comparing the data graphed in Fig. 7, with Figs. 4 and 5. One notes that the data taken in the region of overlap clearly resemble the results predicted in Fig. 4, in which it is assumed that $\nu_{ab} > \nu_b - \nu_a$, rather than the results predicted in Fig. 5, where $\nu_{ab} < \nu_b - \nu_a$ is assumed. The dependence on relative concentration, along with the fact that the two ions were each observed by this optical method to have identical decay characteristics, leads to the conclusion that the Pr:ErES samples have a cross-relaxation rate ν_{ab} , which exceeds the difference between the individual rates $\nu_b - \nu_a$.

Because it was experimentally impossible to detect the faster time constant corresponding to the rate ν_a , it is not possible to completely determine

the cross-relaxation rate ν_{ab} . However, from this experiment one can establish a lower limit $\nu_{ab} > 10^4 \text{ sec}^{-1}$ and conclude that the relaxation of both ions is proceeding at a rate which corresponds to the solution (13a) of the rate equations.

Although data on these two samples with differing relative concentrations of Pr and Er follow quite closely the expected relaxation rates which were graphed in Fig. 4, precise fits are not attempted for the following reasons: (a) Because of segregation during growth, the relative concentrations of Pr and Er in the samples could only be estimated from the optical-absorption strength; and (b) the fact that the relaxation of the isolated praseodymium ion is phonon bottlenecked causes difficulties in estimating the true value of ν_b to use in the evaluation of the rate ν_a . Because the phonon-bottleneck phenomenon is so dependent on the spin bandwidth, the presence of the broad erbium resonance may actually relieve the phonon bottleneck which can inhibit the relaxation of the praseodymium ions.

The data for the Pr:ErES crystal, sample A, were taken with $\theta = 7^\circ$; so the Er resonance was centered on the Pr2 resonance and overlapped the Pr1-Pr3 lines. When the external field was set so that the microwaves pumped any of these three Pr lines, both Er and Pr were observed to have com-

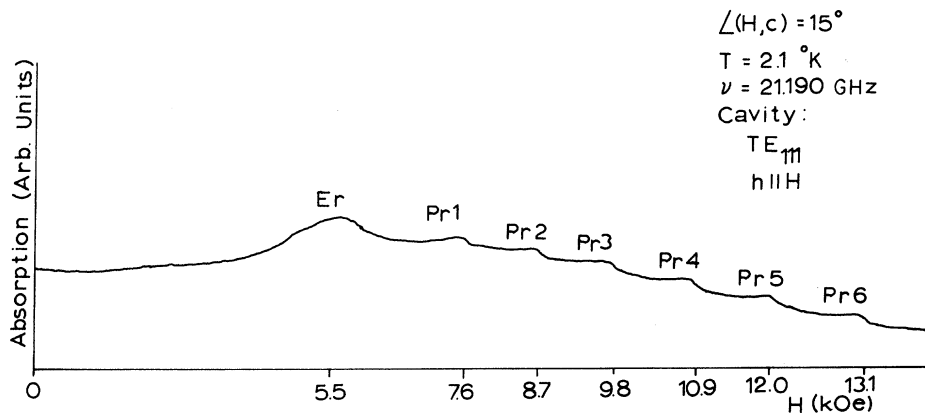


FIG. 9. Microwave-absorption spectrum of the Pr:ErES (1:4) sample B.

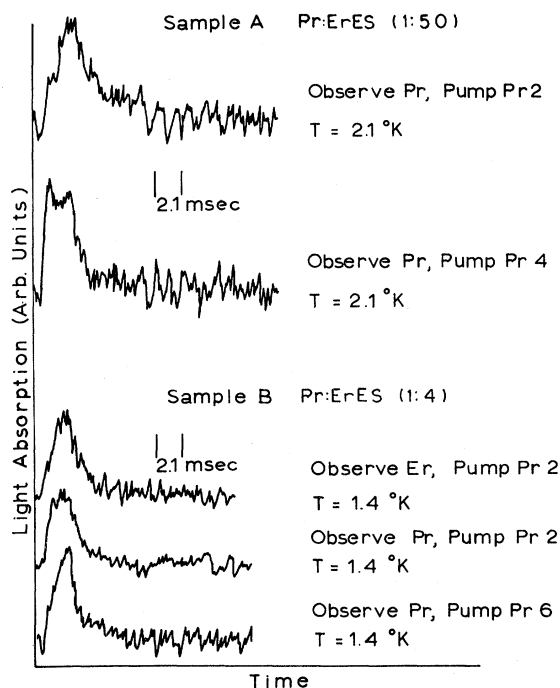


FIG. 10. Experimental-relaxation curves for a few interesting cases, illustrating the relative signal-to-noise ratio of the measurement. In each case shown, the signal was averaged 1024 times.

mon decay time. However, when the field was set so that the microwave fields pumped Pr resonances Nos. 4 and 5, significantly faster relaxation rates were observed for the Pr ions, while negligibly small Er optical signals were encountered. The cross-relaxation equations predict, for a given concentration ratio, a rate gap [$r_+ \leq r_a + (N_b/N_a) \times (r_b - r_a)$ and $r_- \geq r_b$] for any value of r_{ab} . The ex-

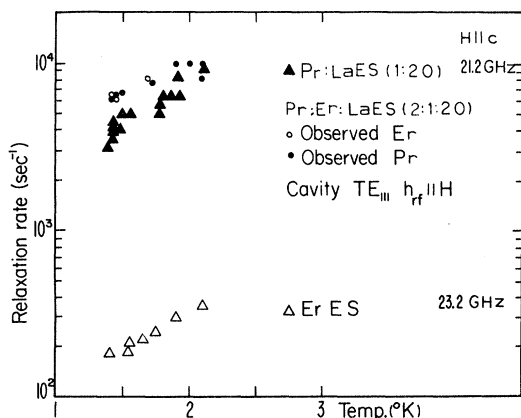


FIG. 11. Temperature dependence of observed relaxation rates in a Pr:Er:LaES (2:1:20) crystal in which the interacting paramagnetic ions are diluted by the presence of diamagnetic-lanthanum ions. Data for samples having only Pr and Er ions are included for reference.

perimental-decay curves do not seem to permit a fit to two allowed rates, and as the apparent relaxation rates for these "isolated" hyperfine lines of Pr fall into the rate gap, they are not understood. A possible explanation of the observed rates may be that they are due to a local clustering of Pr ions in this host crystal.

Figure 10 shows some of the relaxation displays for these samples, which are the traces obtained of the signal-averager output. These decay curves illustrate the relative signal-to-noise ratios obtained for practical averaging times (1000 sweeps) and the variation of signal buildup and decay for a few interesting cases.

Evidence that a relieving of the phonon bottleneck may occur is seen in Fig. 11, which presents the results of measurements made on a Pr:Er:LaES (2:1:20) sample, in which the interacting ions are diluted by the presence of the diamagnetic lanthanum ion. Figure 12 shows the microwave-absorption spectrum for the same crystal, in which the erbium resonance, overlapping Pr5, is observed to be considerably narrower than in the Pr:ErES samples due to the rarity of other erbium ions. The most prevalent ion in this particular sample was praseodymium, and cross relaxation led to extremely rapid relaxation for the erbium ions as expected. The most interesting result, however, is that both the praseodymium and the erbium ions had relaxation rates which were faster than that measured for isolated praseodymium, indicating that the phonon bottleneck had been relieved. In this sample, erbium optical signals were obtained

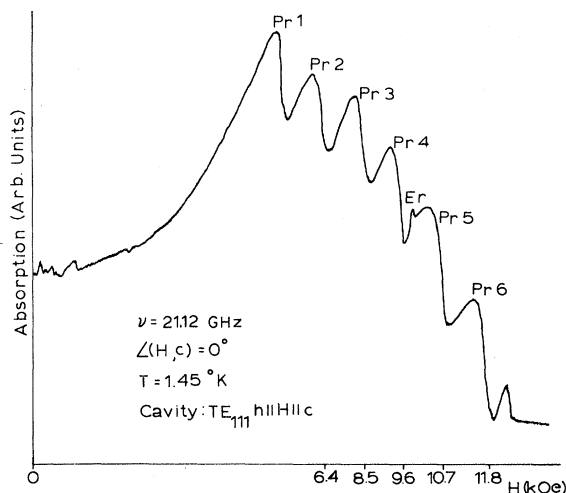


FIG. 12. Microwave-resonance spectrum of the Pr:Er:LaES (2:1:20) sample. The additional line at 12 kOe had the angular dependence of the Pr ion. It is believed to be the $M_I = \frac{5}{2}$ hyperfine line of those Pr ions in the vicinity of Er ions, having a g value of 1.5, characteristic of Pr in ErES, rather than the value 1.69 of Pr in LaES.

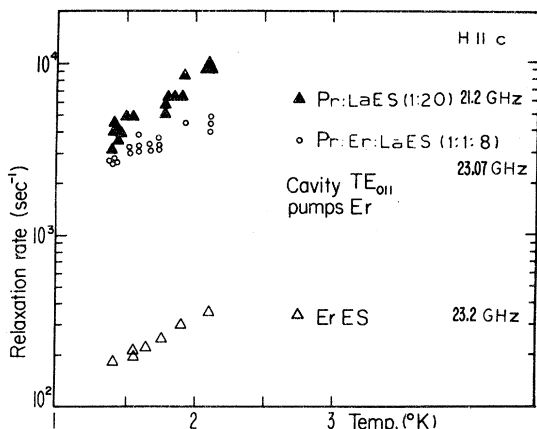


FIG. 13. Temperature dependence of observed relaxation rates in a Pr:Er:LaES (1:1:8) crystal.

even though microwave power was applied at the Pr1 resonance. This indicates that rapid cross-relaxation processes are occurring between the hyperfine lines of Pr in this sample, which has a relatively high concentration of Pr compared to that of the Pr:ErES sample where the data indicate there was isolation of the Pr hyperfine lines from each other.

Figure 13 shows the results of relaxation measurements on a Pr:Er:LaES (1:1:8) crystal. Figures 11 and 13 together illustrate that the Pr and Er ions, even though diluted by the presence of lanthanum ions, are characterized—as is the case for the PrErES samples of Fig. 7—by an interaction strength such that $\tau_{ab} \gg \tau_b - \tau_a$.

In summary, cross-relaxation measurements on praseodymium-erbium-ethylsulfate crystals show that the spin dynamics of these mixed crystals are characterized by a fast cross-relaxation rate, in spite of the absence of an effective magnetic dipole-dipole interaction which vanishes because $g_{\perp} = 0$ for Pr.

Because of the fast isolated relaxation of Pr, the virtual-phonon exchange is expected to be quite strong between Pr ions. Using the estimate (20) for the cross-relaxation rate due to the VPE between Er and Pr, one finds $w_{ij} \sim 7 \times 10^3 \text{ sec}^{-1}$. This is of sufficient magnitude to account for the tightly coupled relaxation behavior of the ions in these mixed crystals when the resonances overlap. Estimates of w_{ij} for these ions are made difficult by the inhomogeneously broadened resonance of the Pr ion.

It is unfortunate that this experiment cannot resolve the controversy as to whether the most important mechanism for energy transfer is the virtual-phonon exchange or electric-multipole interaction, but even a precise value of the cross-relaxation rate would not at present resolve that

point.

In these experiments on Pr-Er cross relaxation, the extent of resonance overlap was found to be an important factor. Samples having low concentrations of Pr (< 10%) exhibited relaxation behavior which indicated only slight-spin communication between different hyperfine lines of Pr. However, samples having higher concentrations of Pr exhibited overlapping hyperfine lines, and the observation of energy transfer to the distant Er resonance indicated that spin energy was transferred along the overlapping hyperfine lines of Pr.

The optical technique allowed complete discrimination of the ions. When microwave power was applied in the region of resonance overlap, optical detection demonstrated that the Er and Pr ions both relaxed with a common rate, thus verifying the predictions of the cross-relaxation-rate equations when $\tau_{ab} > \tau_b - \tau_a$.

B. Cerium-Neodymium Ethylsulfates

Figure 14 shows the angular dependence of the resonances of the lowest crystal field state of neodymium and the two lowest states of cerium ions in the ethylsulfate lattice. In concentrated crystals where the resonances are broad, there is the pos-

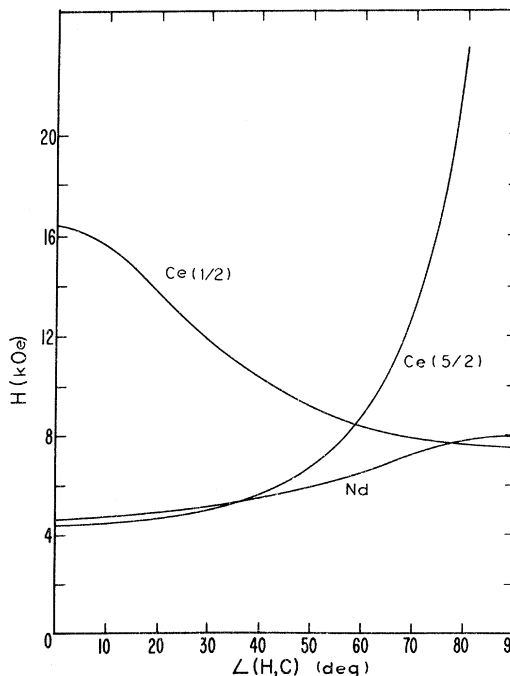


FIG. 14. Predicted angular dependence of the 23.1-GHz paramagnetic-resonance spectrum of Nd and Ce ions in LaES based on g values from Ref. 26. Both ions in the NdES host crystal were found to have states with similar g values. The angular dependence of both crystal field states of Ce which are populated at low temperatures are shown.

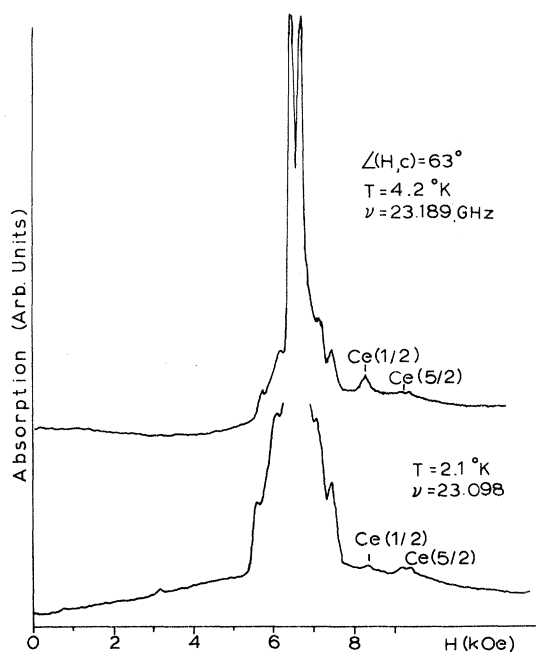


FIG. 15. Microwave-absorption spectra of a Ce:NdES (1:5) crystal at $T=4.2^\circ\text{K}$ and $T=2.1^\circ\text{K}$, from which the separation of the lowest levels of the Ce ion in this crystal was calculated.

sibility of some overlap between the Nd resonance and that of the $\text{Ce}(\frac{5}{2})$ state at $\theta=0$, where the optical method can be used. Prior studies have shown that the two lowest crystal field doublets of cerium in ethylsulfates lie in close proximity to each other.²⁶ In concentrated CeES the $M_j = \frac{5}{2}$ state is the lowest, but in dilute Ce:LaES the $M_j = \frac{1}{2}$ state is the lower of the two. In both salts, the other crystal field doublet is within a few wave numbers (4.6 and 3.9 cm^{-1} for CeES and Ce:LaES, respectively), giving the relaxation of the Ce ion its rapid rate and steep Orbach-process exponential temperature dependence.²²

The absence of optical transitions of Ce in the visible region made it impossible to separately monitor the Ce ground-state populations in mixed salts. Nevertheless, because Ce and Nd have vastly different relaxation rates and their resonances were expected to overlap, cross relaxation was sought by monitoring the behavior of the Nd optical-absorption lines. To keep the rate of relaxation within the capabilities of the signal-averager's time response, it was decided to study salts in which the slower Nd was the more abundant ion; in particular, where Ce was diluted into NdES.

The nature of the EPR of the Ce ion in NdES was unknown prior to this study. In CeES the resonance of the $\frac{5}{2}$ state of Ce is difficult to detect and is seen only at 2.2 °K and below, because it is weak and broad owing to the small g_1 and large inter-

ionic interactions. In the NdES host, however, the EPR is comparatively well behaved and both $\frac{1}{2}$ and $\frac{5}{2}$ states of Ce are clearly seen. Figure 15 shows a display of the microwave-absorption spectrum of Ce:NdES (1:5) at an angle of magnetic field which separates the various resonances. The temperature dependence of the relative strength of the Ce resonances revealed that in this salt the $M_j = \frac{5}{2}$ state of Ce is the lowest, and the $M_j = \frac{1}{2}$ state lies $6.5 \pm 1.0 \text{ cm}^{-1}$ above it. The angular dependence of the lines indicates that the g values of the states are essentially unaltered from their isolated-ion values. Figure 16 shows the structure of the microwave absorption of Ce:NdES (1:5) with the magnetic field parallel to the crystal axis. It exhibits the characteristic triplet structure of the Nd resonance due to differing alignment of nearest-neighbor ions.²⁷ The Ce resonance is seen at 4450 G.

Figure 17 shows the results of relaxation measurements on NdES, Nd:LaES, and Ce:NdES (1:10), where the numbers in parentheses are the relative concentrations of the ions.

The Nd samples which had no added Ce impurity, exhibited relaxation rates which were a factor of 3 slower than the rate predicted by extrapolating the Scott and Jeffries²² results by the ω^4 dependence of the direct process. This is a disappointing result, considering the closer agreement obtained for the erbium ion. The comparatively large linewidth of erbium makes it more immune to phonon-bottleneck complications.

The phonon bottleneck was clearly evident in the studies of NdES where its decay curve could be drastically altered from that of a single exponential by using microwave powers above 25 mW. Under these circumstances, the decay curve could be characterized within experimental error as the sum of two exponentials whose rates are shown in Fig. 17 connected by a vertical line. It was disappointing to find that the characteristics of the nonexponential decay of Nd did not completely correspond to the predictions of the Faughnan and Strandberg²³ treatment of the phonon bottleneck discussed in Sec. III. Although the departures from exponentiality had the order of magnitude predicted for $\sigma \approx 2$, the initial decay rate was found to be faster than τ^{-1} , in contradiction to the predictions of the theory.

The relaxation of the isolated cerium ion in these mixed samples could not be directly measured with an optical technique. One expects the Ce rate to be similar to that reported by Scott and Jeffries²² on the relaxation of the $M = \frac{1}{2}$ doublet of 0.2-at. % Ce in LaES, i. e., the $\frac{5}{2}$ state of the cerium ion in NdES is expected to have a very fast Orbach-process relaxation because of the presence of the higher-lying $M_j = \frac{1}{2}$ state, which was seen in the

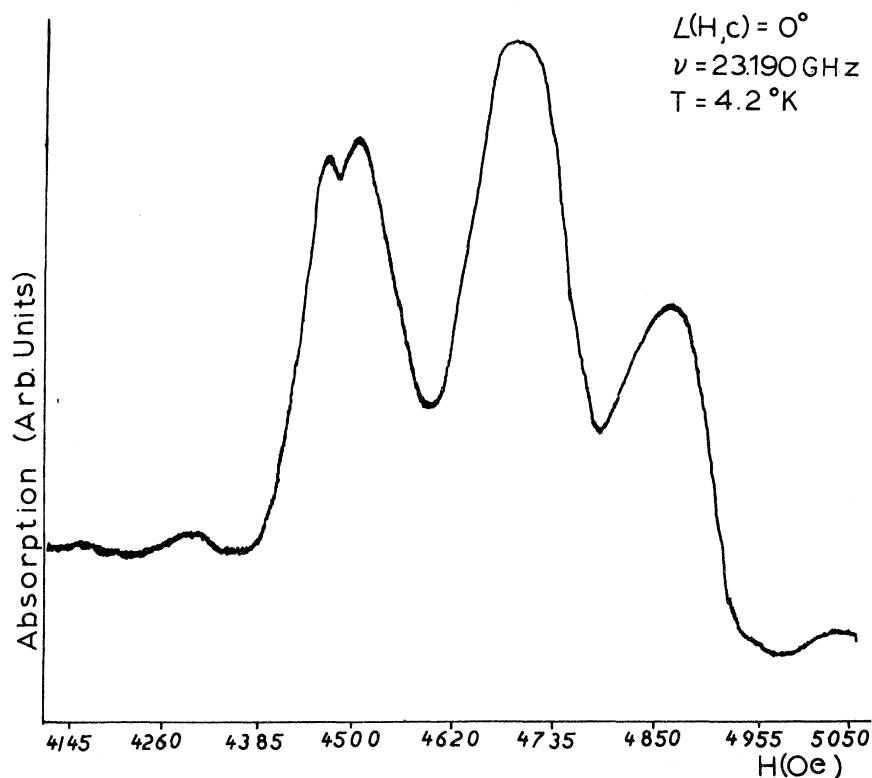


FIG. 16. Microwave-absorption spectrum of Ce:NdES (1:5) crystal. The $\text{Ce } (\frac{5}{2})$ resonance is seen at 4450 Oe.

EPR spectrum.

Interesting behavior for mixed samples of Ce:NdES is seen in Figs. 17-19 for samples with concentration ratios of (1:10), (1:20), and (1:5). The temperature dependence of the unbottlenecked

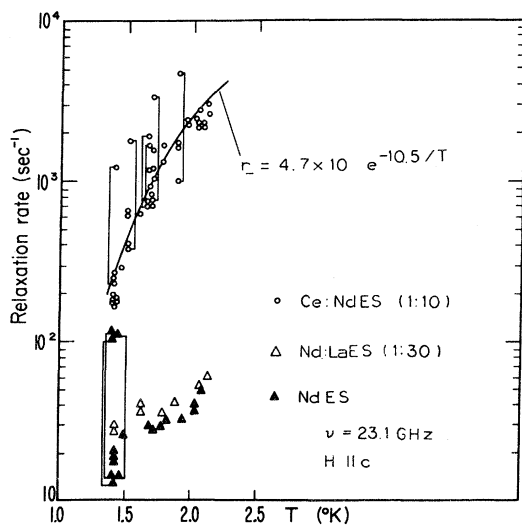


FIG. 17. Temperature dependence of observed relaxation rates in Ce:NdES (1:10), NdES, and Nd:LaES (1:30) crystals. Nonexponential-decay curves were fit to a sum of two exponentials having rates which are represented by the data points connected by vertical bars. Nonexponential decays only occurred at large pump powers.

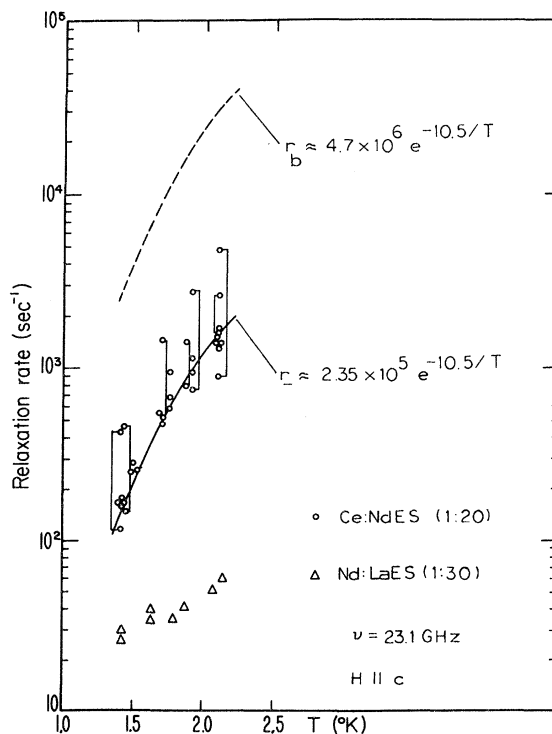


FIG. 18. Temperature dependence of observed relaxation rates in a Ce:NdES (1:20) crystal. Nonexponential decays are again indicated by vertical bars. The broken curve indicates the relaxation rate a noninteracting Ce ion would have in this host crystal.

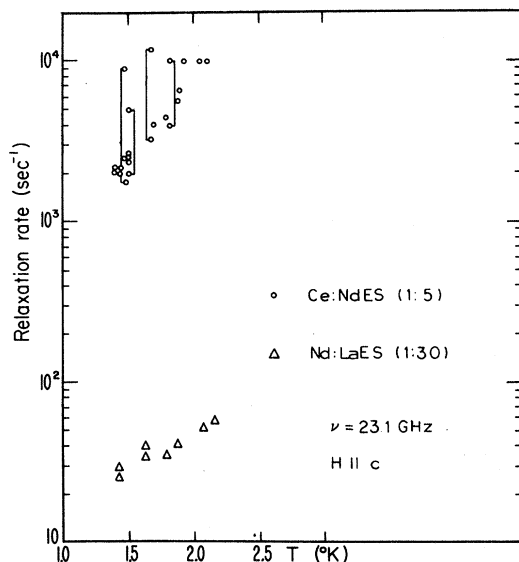


FIG. 19. Temperature dependence of observed relaxation rates in a Ce:NdES (1:5) crystal.

data points indicates that the neodymium ions are relaxing with a steep temperature dependence which scales as the ratio of the Ce:Nd concentration. The data for the (1:10) and (1:20) samples appear to fit a curve of the form $R \propto e^{-10.5/T}$, which predicts a level at 7.3 cm^{-1} above the ground state—in good agreement with the value estimated from the temperature dependence of the EPR. Using Eq. (13a), one can predict from these samples the rate r_b which would characterize the relaxation of an “isolated” Ce ion in the NdES lattice. Such an analysis predicts a relaxation rate for Ce in this crystal, $R_{\text{Ce}} = 4.7 \times 10^8 e^{-10.5/T}$.

The data for the Ce:NdES (1:5) samples could not be fit to a curve with the same slope, demonstrating instead a flatter temperature dependence. This may be due to the onset of heat-flow limitations due to the establishment of a Kapitza-resistance layer at the crystal-liquid-helium interface. Effects of this phenomenon have been seen by Griffiths and Glattli²⁸ and Glattli²⁹ using Faraday-rotation methods to measure the relaxation of CeES samples of larger sizes than those studied here. They found that the relaxation rates for ions in their samples could be explained in terms of a theory of heat flow across the Kapitza layer. When Glattli measured the relaxation of the $\text{Ce}(\frac{5}{2})$ state in CeES, he found the relaxation to be much slower and flatter than that expected from spin-lattice relaxation theory, but which could be understood in terms of Kapitza resistance.

The data of this study on mixed samples of Pr:ErES and Ce:NdES scale with concentration as predicted by Eq. (15), and usually have a temperature dependence in agreement with spin-lattice

relaxation theory without consideration of Kapitza resistance. Hence, Kapitza-resistance limitations appear to be generally absent from samples of the size used here ($2 \times 2 \times 1 \text{ mm}$). However, deviations from expected behavior for samples having relaxation rates of 10^4 sec^{-1} may signal the first occurrence of heat-flow problems from the crystal to the bath.

The relaxation curves of the mixed samples of Ce:NdES showed, in many cases, a rapid initial decay, followed by a slower relaxation. Such curves, when plotted on semilog paper, were fit within experimental error to a sum of two exponentials having rates which are represented by the data points connected by vertical bars. In each case, the magnitude of the fast exponential had the same sign and was approximately one-fourth the magnitude of the slow exponential. Efforts were made to isolate the parameters upon which this nonexponential decay depended. There was no clear correlation with the position on the resonance curve at which microwave power was applied, but the phenomenon occurred only with large pump powers. Because of the averaging process, analog methods of analyzing the relaxation curve while taking data were prohibited, so the nonexponentiality only became apparent after replotting the data on semilog paper. The scatter of points is believed due to the difficulty in fitting two time constants to a fairly noisy signal.

In cross-relaxation experiments, the natural assumption is that the two time constants represent the rates r_+ and r_- of the coupled-ion rate equations. However, such an association is not believed to be justified. The faster of the experimental time constants is not sufficiently fast to represent the faster rate r_+ of the rate equations. Further, if the phenomenon were associated with cross relaxation, it should depend on the location on the resonance-absorption spectrum at which pump power was applied.

In their experiments on Ce-Er cross relaxation in LaES crystals, Larson and Jeffries⁴ found compound relaxations which were related to both a fast and a slow cross relaxation occurring between the Er and the two states of the Ce ion, respectively. The situation is different for this experiment, as the separation between the Nd resonance and the $\text{Ce}(\frac{1}{2})$ resonance is larger and the greater splitting between the Ce states in this crystal reduces the number of Ce ions in the $\text{Ce}(\frac{1}{2})$ state as compared to their crystal. Thus cross relaxation between Nd and $\text{Ce}(\frac{1}{2})$ is expected to be negligible.

As the nonexponential decays were independent of the position at which the microwave resonance was pumped, and because they occurred only at large pump powers, it was concluded that they are associated with a phonon bottleneck. Analysis of the

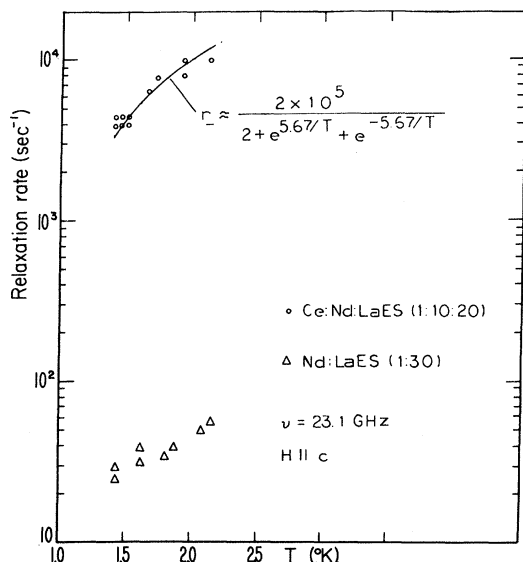


FIG. 20. Temperature dependence of observed relaxation rates in a Ce:Nd:LaES (1:10:20) crystal. The temperature dependence reflects the altered level separation of the Ce ion in LaES contrasted with its separation in the NdES crystal. In this sample, cross relaxation occurs between the Nd ions and those Ce ions in its first excited state.

phonon bottleneck in this case is complicated by the presence of two different ions, and by the fact that one of them (Ce) is relaxing by an Orbach process rather than by the direct process. As the relaxation rate for the two ions given by Eq. (13a) has its dominant contribution from the Ce ion, we must assume that it is the Ce ion which is bottlenecked. Scott and Jeffries²² have briefly discussed the phonon-bottlenecked Orbach process and predicted a bottlenecked rate having an exponential temperature dependence like that of the unbottlenecked ion. The data for the longer-time constant correspond to this; however, the full explanation of the departure from single-exponential decay probably lies, as in the case of the bottlenecked direct process, in consideration of the nonlinear equations.

Because of the broadband nature of the optical method used here, spin diffusion can be definitely ruled out as a source of the rapid initial decay. It is apparent that although experiments on mixed crystals offer a convenient means for studying the phonon bottleneck as a function of a variable spin-lattice relaxation time, it is complicated because the linewidths vary with concentration. Furthermore, analysis is made difficult when relaxation proceeds via different mechanisms in different ions.

Effects of dilution were investigated using samples in which the Ce and Nd paramagnetic ions are diluted in lanthanum ethylsulfate. The temperature dependence of the relaxation rate by Eq. (13a) might at first be expected to differ from the Ce:NdES case because, when diluted in LaES, the state of

the Ce ion, which has approximately the same splitting as the Nd ions, is now the excited state at 3.94 cm^{-1} ($5.67 \text{ }^\circ\text{K}$), and its population is a rapidly varying function of temperature encountered in this experiment. However, the population effect is exactly balanced by the change in the Orbach-process relaxation rate⁴; so that the cross-relaxation solution for case I, Eq. (13a) predicts, as was the case for Ce:NdES, a rate which varies with temperature according to the expression $r \propto (2 + e^{\Delta/kT} + e^{-\Delta/kT})^{-1}$.

Figures 20 and 21 show the results of measurements made on Ce:Nd:LaES samples with relative concentrations of (1:10:20) and (0.5:10:20). The data reported here show good agreement with the expected temperature dependence. It is apparent from the rapid-relaxation rates of the neodymium ions that the cross-relaxation rate is again very fast, in spite of the dilution.

The magnetic-dipole interaction between Ce and Nd (Table I) is of sufficient strength to account for the rapid cross-relaxation rate, which can be inferred from the data for the Ce-Nd ethylsulfates.

C. Relaxation of CeES: Faraday Rotation

Figure 22 shows measurements of the relaxation of CeES taken by means of Faraday-rotation methods. Such measurements on CeES have already been reported by Glatli,²⁹ who found anomalously slow rates ($1/\tau \approx 300 \text{ sec}^{-1}$) instead of the rapid Orbach-process rates which one would expect from the electronic-level structure of the Ce ion in this crystal. Glatli's data are explained in terms of Kapitza resistance to heat flow across the crystal surface having a time constant $\tau = MCR/S$, where M

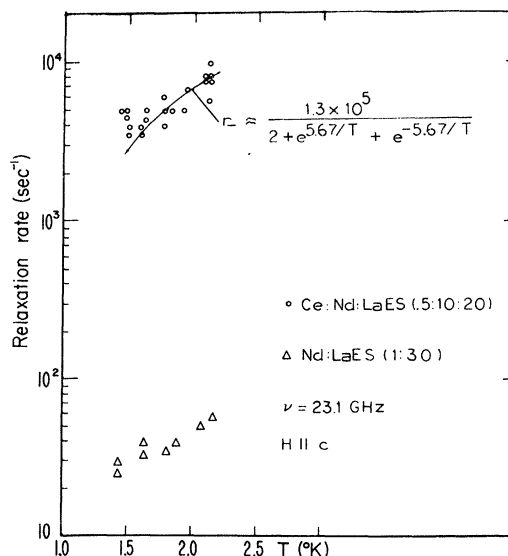


FIG. 21. Temperature dependence of observed relaxation rates in a Ce:Nd:LaES (0.5:10:20) crystal.

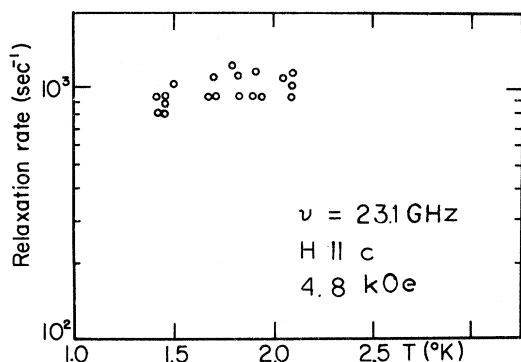


FIG. 22. Temperature dependence of observed relaxation rates in a CeES crystal as measured by Faraday-rotation methods. Sample size was $3 \times 2.5 \times 1$ mm.

is the mass, C is the specific heat, S is the surface area, and R is the Kapitza resistance. Measurements of the relaxation of CeES were repeated here because it was wondered why similar Kapitza-resistance difficulties were not manifest in some of the data obtained in the present study of crystals with the same ionic concentration. If present, the Kapitza resistance should have severely limited the relaxation rates of those crystals with the larger-concentration ratios of fast-relaxing to slow-relaxing ions. In particular, the similarity of the Ce:NdES level structure to that of CeES suggests that it might be expected to exhibit similar "Kapitza-limited-"relaxation behavior.

The data taken here on CeES shown in Fig. 22 are a factor of 3 faster than the rates reported by Glatli, but exhibit a temperature dependence and an unexpectedly slow rate in agreement with his analysis. The difference in rates may be due to the different crystal sizes studied, or to the different microwave frequencies used to heat the samples.

It is apparent from this data that the Kapitza limitation of CeES relaxation is much more severe than in any of the other samples studied. The data on the Ce:NdES samples suggest that the Kapitza problem is not generally encountered there, except perhaps in the Ce:NdES (1:5) sample, where the expected temperature dependence was not observed. Apparently, the presence of the slower-relaxing neodymium ions and the smaller specific heat is sufficient to relieve the Kapitza limitations for these mixed samples, and the relaxation behavior is governed by properties intrinsic to the crystal. This measurement shows that Kapitza resistance still is the dominant factor in determining the relaxation rate of CeES for the small sample size and the higher frequencies used in this study. It is a factor which must be kept in mind in interpreting the results of relaxation measurements.

D. Praseodymium-Nickel Double Nitrate

The double-nitrate crystal $\text{La}_2\text{Mg}_3(\text{NO}_3)_{12} \cdot 24\text{H}_2\text{O}$ (LaMN) containing praseodymium and nickel ions can be expected to exhibit cross relaxation because of overlapping resonances. Figure 23 is a plot of the magnetic splitting of these ions as a function of magnetic field for H parallel to the crystal axis. One notes the possible overlap between the Ni resonance and the Pr resonance near 9 kOe. Figure 24 illustrates some microwave-absorption spectra taken here on various crystals containing Pr and Ni. The EPR of the dilute-nickel salt shows the expected resonances, and the PrMN crystal exhibits the characteristic six hyperfine lines. The magnetic-resonance spectrum of the concentrated-nickel salt shows a very broad pattern which is probably due to the presence of other nickel neighbors. Such a spectrum overlaps greatly with that of the praseodymium ion when the ions are mixed to form the Pr-Ni double-nitrate crystal. As the g_1 of Pr in this salt is zero, it appears at first sight to be an interesting case to study for cross relaxation.

The optical spectrum of Ni in this crystal exhibited very broad absorptions in the red, which serve to give the crystal its deep-green hue. Unfortunately, the optical-absorption strength was quite small. Crystals whose microwave absorption was large enough to completely destroy the cavity resonance exhibited peak optical absorptions of only 10%, far from the optimum for best signal to noise. The Pr ions similarly exhibited a weak optical absorption. Nevertheless, relaxation mea-

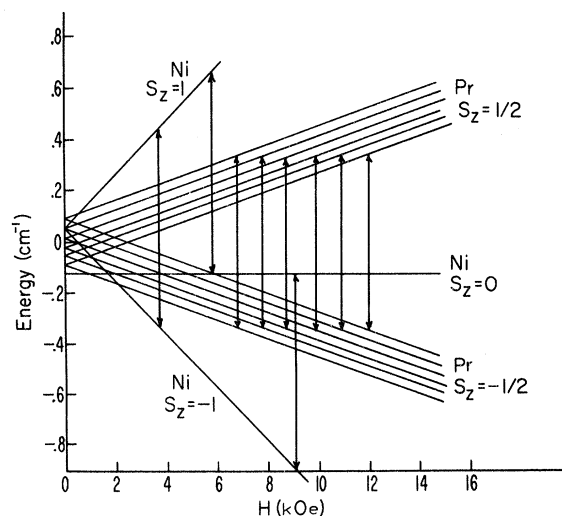


FIG. 23. Predicted magnetic splitting of Ni^{2+} and Pr^{3+} ions in the double-nitrate crystal for $H \parallel C$ based on g values from Ref. 26. Transitions for 23.2-GHz microwaves are indicated by vertical arrows.

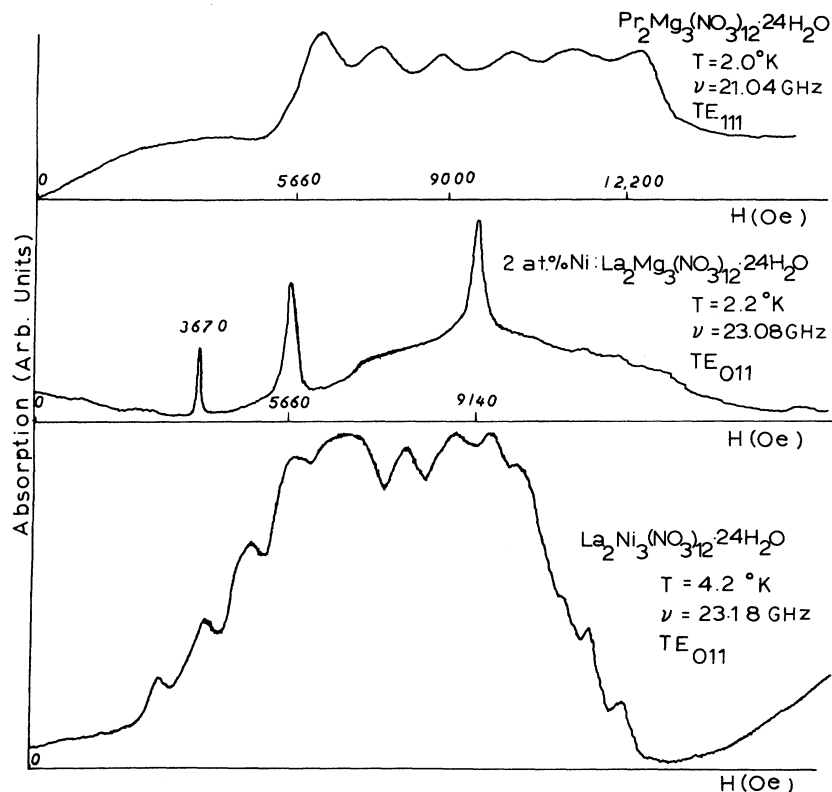


FIG. 24. Microwave-resonance spectra of some Ni and Pr double-nitrate crystals.

surements could be obtained with difficulty for concentrated crystals.

The results of relaxation measurements on mixed and unmixed salts are presented in Fig. 25. The relaxation rate of the concentrated praseodymium salt is approximately the same as that measured by Scott and Jeffries²² on a 1-at.% Pr in LaMN crystal at 9.15 GHz and has a slope which indicates it is phonon bottlenecked. The relaxation rate of the nickel double nitrate was unknown prior to these measurements. When measured here, the nickel ion was found to have a relaxation rate almost the same as that of the praseodymium ion. This re-

sult is disappointing from the standpoint of studying cross relaxation, for in such a case the presence of the interactions between the ions does not affect their relaxation behavior. Measurements of the relaxation of the mixed salt confirmed this.

E. Praseodymium-Samarium Ethylsulfate

The samarium ion in the lanthanum ethylsulfate crystal has $g_{\parallel} = 0.596$ and $g_{\perp} = 0.604$.²⁶ Hence, for H parallel to the crystal axis and at the microwave frequencies used here, the Sm ion is expected to have a magnetic splitting which is roughly one-half as large as that of the $M_I = \frac{5}{2}$ hyperfine line of the

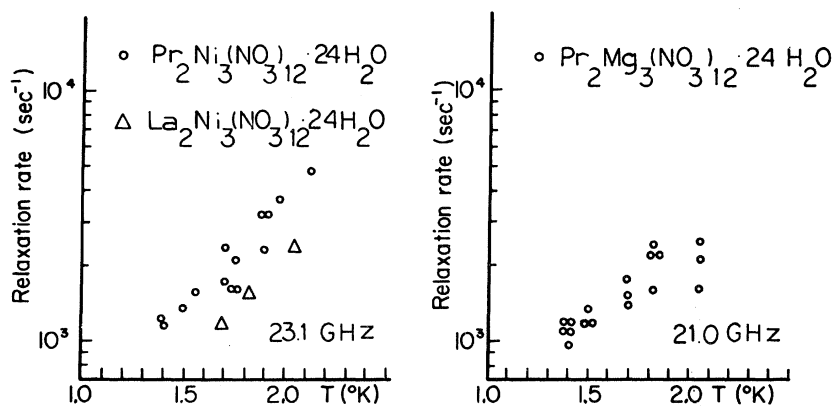


FIG. 25. Temperature dependence of observed relaxation rates in some Ni and Pr double-nitrate crystals.

praseodymium ion. These ions can be investigated for a cross-relaxation process which involves the exchange of magnetic energy between two Sm ions and one Pr ion.

Larson and Jeffries³⁰ found the relaxation rate of the samarium ion in LaES to be very slow in the temperature range of interest, having a rate of only $1/\tau = 1.5 \text{ sec}^{-1}$ for $T = 1.4 \text{ }^\circ\text{K}$, $\nu = 9.36 \text{ GHz}$, and $\vec{H} \parallel \vec{C}$. This contrasts with the Pr ion, which has a rate of $\approx 10^4 \text{ sec}^{-1}$; hence, the occurrence of cross relaxation should drastically affect the relaxation rates of both ions.

Experiments were made on a sample of $\text{Pr}_{0.03}\text{Sm}_{0.97}\text{ES}$ in both the TE_{011} and TE_{111} cavities. In this Sm-rich crystal, it was hoped that the Sm resonance would be broad enough to allow spin-exchange transitions with the Pr ion.

Unfortunately, no cross-relaxation effects were observed in this sample. The Pr ions exhibited their characteristically fast relaxation, and no signal could be found on the Sm optical-absorption lines in response to the Pr ions being pumped by microwave pulses. If cw microwave power is used, capacitive smoothing of the photomultiplier output allows significant reduction of noise, and the absorption of circularly polarized light can be used to observe the absorption of cw microwave power by either ion as a function of field. Such a procedure using one of the Pr-optical-absorption lines resulted in a spectrum reproducing the six hyperfine lines in the microwave-absorption spectrum of Pr. Interaction between the ions was sought by monitoring the Sm optical absorption while the field was swept through the Pr resonances, but no signal was observed. This result showed that pulsed experiments to seek cross relaxation had little prospect of success.

The EPR of the Pr ion in SmES was measured here and is characterized by the spin-Hamiltonian parameters $g_{\parallel} = 1.55$ and $A = 0.073$. These parameters differ somewhat from the values reported for Pr:LaES of $g_{\parallel} = 1.69$ and $A = 0.88$.¹⁰

Cross relaxation may not have been observed in this system for a number of reasons. In the first place, $g_{\perp}(\text{Pr}) = 0$, so the dipolar interaction vanishes. Second, these ions can only cross relax through a higher-order process in which each Pr ion exchanges energy with two Sm ions. Finally, neither the breadth of the samarium resonance nor the extent of its energy "overlap" with the Pr levels is known with exactitude in this experiment because the Sm resonance was not observed, its position being expected at 27.6 kOe, which is beyond the limit of the magnet to achieve. However, observation of the half-field resonance of Sm would give information on its breadth. In the other concentrated crystals studied here (the ErES and NdES), the half-field resonance could be clearly observed, but

no evidence of the Sm-half-field resonance was observed when it was sought using a TE_{011} cavity. This is likely owing to the relatively small value of g_{\perp} of this ion which causes the dipolar interaction to be less effective in mixing states. This small value of g_{\perp} would lead one to expect a comparatively narrow resonance line as well.

Any future study of this system should be done with a microwave frequency which guarantees more complete overlap, and which allows observation of the Sm-full-field resonance.

V. SUMMARY AND CONCLUSIONS

These experiments have shown that the optical-microwave technique can be used to investigate the phenomenon of cross relaxation in mixed crystals, where it has the advantage that it can discriminate between ions even when the microwave resonances overlap.

It has been found here in the case of overlapping resonances in Pr:Er ethylsulfates that, in spite of the absence of the magnetic dipole-dipole interaction, the other interactions are still sufficiently strong to give cross-relaxation rates which are faster than individual-ion relaxation rates. As predicted by the rate equations for such a circumstance, both ions were observed to relax with a common rate which was intermediate between the two isolated-ion relaxation rates. Estimates of the cross-relaxation times due to nondipolar interactions indicate that even these very weak ($\sim 10^{-4} \text{ cm}^{-1}$) interactions are sufficiently strong to account for the observed behavior.

In general, it was found that the spin dynamics of ions having overlapping resonances were accurately predicted by the solutions of the cross-relaxation-rate equations in which the cross-relaxation rate is taken to be much faster than the isolated-ion relaxation rates. The independence of relaxation rates on position within the microwave-absorption spectrum at which microwave power was applied leads to the qualitative conclusion that spin energy is transferred rapidly throughout the linewidth and, in turn, to the ion of a different species which has a partially overlapping resonance.

It was found that dilution of the samples with diamagnetic ions did not diminish the cross-relaxation rate to an extent that it could be directly measured. The weak optical-transition strength, however, limited the extent to which the samples could be diluted.

Phonon-heating effects resulted, in the case of the Ce-Nd ethylsulfates, in a pronounced nonexponentiality in the decay curve when high powers were used. None of the existing theories of the phonon bottleneck were found to adequately explain the details of the curve. The anomalously slow relaxation rate of the Ce ion in CeES indicates

that problems associated with heat flow to the bath are eventually encountered in cases where the spin-lattice relaxation rates are fast and the specific heat of the sample is large.

In most cases, phonon heating was not a problem, and the relaxation rates of the ions were determined by properties intrinsic to the ions in the crystal. For example, in the case of Ce: NdES, the temperature dependence of the relaxation rate was used to verify the Ce-level structure suggested by EPR measurements.

The optical technique has some advantages and some disadvantages. As the optical absorption is affected by all of the ions of a given type, the optical method monitors the relaxation behavior only, and is free of cross-relaxation effects which dis-

tribute energy within the paramagnetic-resonance linewidth of a given type of ion—for instance, cross relaxation between the hyperfine lines. This assists in ruling out cross relaxation to hyperfine lines as the source of compound-relaxation decay curves, a conclusion not possible in the case of microwave detection of relaxation. The disadvantages of the optical technique lie in the inherent-shot noise, and in the restrictions upon the crystal orientation and optical-absorption strength necessary for its use which limit the circumstances under which it can be applied. In spite of these limitations and difficulties, the optical technique has shown here its utility in the study of cross relaxation where it does not require bimodal cavities and can distinguish between ions.

*Research supported in part by the National Science Foundation.

¹N. Bloembergen, S. Shapiro, P. S. Pershan, and J. O. Artman, *Phys. Rev.* **114**, 445 (1959).

²G. Feher and H. E. D. Scovil, *Phys. Rev.* **105**, 760 (1957); A. A. Manenkov and A. M. Prokhorov, *Zh. Eksp. Teor. Fiz.* **41**, 71 (1961) [*Sov. Phys. JETP* **15**, 54 (1962)].

³A. Rannestad and P. E. Wagner, *Phys. Rev.* **131**, 1953 (1963).

⁴G. H. Larson, and G. D. Jeffries, *Phys. Rev.* **145**, 311 (1966).

⁵P. R. Solomon, *Phys. Rev.* **152**, 452 (1966).

⁶C. K. Asawa and R. A. Satten, *Phys. Rev.* **127**, 1542 (1962); *Proceedings of the International Conference on Electronic and Magnetic Resonances and Relaxation, Eindhoven* (North-Holland, Amsterdam, 1962).

⁷W. H. Culver, R. A. Satten, and C. R. Viswanathan, *J. Chem. Phys.* **38**, 775 (1963).

⁸J. Wooldridge, *Phys. Rev.* **185**, 602 (1969).

⁹C. A. Moore, dissertation (UCLA, 1971) (unpublished).

¹⁰B. Bleaney and K. D. Bowers, *Proc. Phys. Soc. (London)* **A65**, 667 (1952); B. Bleaney and H. E. D. Scovil, *Phil. Mag.* **43**, 999 (1952).

¹¹I. Svare and G. Seidel, *Phys. Rev.* **134**, A172 (1964).

¹²J. Dweck and G. Seidel, *Phys. Rev.* **146**, 359 (1966).

¹³J. M. Baker, *Phys. Rev.* **136**, A1341 (1964).

¹⁴J. M. Baker, *Phys. Rev.* **136**, A1633 (1964).

¹⁵J. M. Baker and A. E. Mau, *Can. J. Phys.* **45**, 403 (1967).

¹⁶F. I. B. Williams, *Proc. Phys. Soc. (London)* **91**, 111 (1967).

¹⁷R. Finkelstein and A. Mencher, *J. Chem. Phys.* **21**, 472 (1953).

¹⁸B. Bleaney, *Proc. Phys. Soc. (London)* **77**, 113 (1961).

¹⁹W. P. Wolf and R. J. Birgeneau, *Phys. Rev.* **166**, 376 (1968).

²⁰R. Orbach and M. Tachiki, *Phys. Rev.* **158**, 524 (1967).

²¹R. Orbach, *Proc. Roy. Soc. (London)* **A264**, 485 (1961).

²²P. L. Scott and C. D. Jeffries, *Phys. Rev.* **127**, 32 (1962).

²³B. W. Faughnan and M. W. P. Strandberg, *J. Phys. Chem. Solids* **19**, 155 (1961).

²⁴A. M. Stoneham, *Proc. Phys. Soc. (London)* **86**, 1163 (1965).

²⁵J. M. Baker and B. Bleaney, *Proc. Roy. Soc. (London)* **A245**, 156 (1958).

²⁶K. D. Bowers and J. Owen, *Rept. Progr. Physics* **18**, 304 (1955).

²⁷B. Bleaney, R. J. Elliott, and H. E. D. Scovil, *Proc. Phys. Soc. (London)* **A64**, 933 (1951).

²⁸D. J. Griffiths and H. Glatli, *Can. J. Phys.* **43**, 2361 (1965).

²⁹H. Glatli, *Can. J. Phys.* **46**, 103 (1968).

³⁰G. H. Larson and G. D. Jeffries, *Phys. Rev.* **141**, 461 (1966).